The Astronomical Journal, 136:2350–2358, 2008 ??? doi:10.1088/0004-6256/136/6/2350

A SPECTRAL LINE SURVEY OF CRL 2688 IN THE RANGE OF 85–116 GHz

J. A. Park[1], Se-Hyung Cho[2], Chang Won Lee[3], and J. Yang[1]
[1] Department of Physics, Ewha Womans University, Daehyundong, Sedaemun, Seoul 120-750, Korea; jongae.park@samsung.com, jyang@ewha.ac.kr
[2] Korean VLBI Network, Korea Astronomy and Space Science Institute, P.O. Box 88, Yonsei University, 134 Sinchon, Seodaemun, Seoul 120-749, Korea; cho@kasi.re.kr
[3] International Center for Astrophysics, Korea Astronomy and Space Science Institute, 61-1, Hwaam, Yuseong, Daejeon 305-348, Korea; cwl@kasi.re.kr
Received 2007 April 2; accepted 2008 September 27; published 2008 November 10

ABSTRACT

A spectral line survey of the proto-planetary nebula CRL 2688 was carried out in the frequency range of 85–116 GHz with the 14 m radio telescope at the Taeduk Radio Astronomy Observatory. Eight detected molecules are all carbon bearing molecules: HCN, HNC, C_2H, HC_3N, CS, CCS, CN, and CO, and their isotopic species $H^{13}CN$ and ^{13}CO. A CCS line was newly detected in CRL 2688. The molecular lines detected in CRL 2688 were also compared with those of the proto-typical AGB star IRC +10216. The SiS ($J = 5$–4, $v = 0$) molecular line detected in IRC +10216 was not detected in CRL 2688, indicating a lower abundance of the SiS molecule in CRL 2688 than in IRC +10216. Excitation temperatures and column densities of HC_3N in both CRL 2688 and IRC +10216 were derived using standard LTE rotational diagram analysis. The HC_3N column density of CRL 2688 was found to be lower than that of IRC +10216. This fact, together with the lower abundance of the SiS molecule in CRL 2688, may be related to the chemical evolution of the circumstellar envelope of CRL 2688.

Key words: circumstellar matter – ISM: molecules – planetary nebulae: individual (CRL 2688) – stars: late-type

Online-only material: color figures, extended figure

1. INTRODUCTION

In the later stage of stellar evolution, low- and intermediate-mass stars evolve through the asymptotic giant branch (AGB) to planetary nebulae (PNs). In the AGB stage, a mass loss through stellar winds produces an extended circumstellar envelope which becomes a rich source of various molecular species. Molecular line surveys have been very well documented in the case of IRC +10216, the proto-typical carbon-rich AGB star. These are the 3–4 mm Onsala Survey (Johnansson et al. 1985), the 0.8 mm James Clerk Maxwell Telescope (JCMT) and Caltech Submillimeter Observatory (CSO) Surveys (Avery et al. 1992; Groesbeck et al. 1994), the 6–10 mm Nobeyama 45 m Telescope Survey (Kawaguchi et al. 1995), and the 1.7–2.3 mm IRAM 30 m Telescope Survey (Cernicharo et al. 2000). So far, more than 53 molecular species have been detected in this object.

In the post-AGB stage, a star becomes a proto-planetary nebula (PPN), a transitional phase between the end of the AGB and the beginning of the PN phase. During the PPN phase, a large UV field arises from the central star, and high-velocity winds appear and interact with the AGB remnant (Kwok 2000). Observations have indicated that molecular gas continues to exist in the shells (Fukasaku et al. 1994; Bachiller et al. 1997; Highberger et al. 2003). But the chemical composition strongly changes during this stage. Molecular ions start to form during the PPN phase, and CN and HNC increase in abundance. In addition, O-bearing molecules can be formed in carbon-rich objects (Herpin & Cernicharo 2000).

The best studied PPN at millimeter wavelengths is the proto-typical PPN CRL 618. Pardo et al. (2007b) have performed a molecular line survey with the IRAM-30 m telescope in the frequency ranges 80.25–115.75 GHz, 131.25–179.25 GHz, and 204.25–275.25 GHz. The usefulness of HC_3N as a molecular probe in this object has been also reported by Wyrowski et al. (2003); Pardo et al. (2004), and Pardo & Cernicharo (2007a). Sanchez-Contreras et al. (2004) have presented high angular resolution maps of the HCO^+ $J = 1$–0, HCN $J = 1$–0, and millimeter-wave continuum emission using the millimeter-wave interferometer of the Owens Valley Radio Observatory. These HCO^+ and HCN molecules were present in both the slowly and rapidly outflowing components of the envelope of CRL 618. In addition, Cernicharo et al. (2001) have found the first evidence for aromatic molecules seen outside the solar system from the Infrared Space Observatory data of CRL 618.

CRL 2688, the so-called "Egg Nebula," is known to be a PPN which exhibits a bipolar reflection nebula with multiple expanding winds (Sahai et al. 1998; Cox et al. 2000). The central object is an evolved star with a spectral type of F5. The distance is known to be 1 kpc (Ney et al. 1975). There have been numerous line observations toward this source. Documented lines include NH_3, HC_3N, HC_5N (Jewell & Snyder 1984), HC_7N, and HC_9N (Truong-Bach et al. 1988, 1993), SiO, SiC_2, and CN (Bachiller et al. 1997a, 1997b), SiS, C_2H, C_4H, and C_3N (Lucas et al. 1986), and high resolution CO mapping (Cox et al. 2000). However, these observations were each limited to selected molecules. This fact led us to make the unbiased molecular line survey toward this object. This survey of CRL 2688 is a series of 100/150 GHz band line surveys with the 14 m telescope at the Taeduk Radio Astronomy Observatory (TRAO) which has produced published results in the surveys of Orion KL (Lee et al. 2001; Lee & Cho 2002) and G34.3+0.3 (Kim et al. 2000, 2001).

We present in this paper a spectral line survey toward CRL 2688 from 85 GHz to 116 GHz, together with several selective line observations in the 2 mm band using the TRAO 14 m radio telescope. We also compare these observational results from CRL 2688 with those from IRC +10216, which represent a different stellar evolutionary stage. The observations are described in Section 2. The results and

discussion are presented in Section 3. The conclusions are given in Section 4.

2. OBSERVATIONS

The observations were performed with the TRAO 14 m radio telescope from 1999 February to May. The half-power beam width (HPBW) of the antenna varies from 64″ to 46″ over the frequency range of 80–150 GHz. The main beam efficiencies of the telescope were measured to be 0.39 at 146 GHz and 0.5 at 86 GHz, respectively (Park et al. 1997). A frequency-unbiased survey ranged from 85 to 116 GHz was conducted using the 100/150 GHz band dual channel SIS receiver which had been developed for simultaneous observations of the 3 mm and 2 mm bands (Park et al. 1999). The single sideband system noise temperatures typically ranged from 240 to 450 K in the frequency range of 85–114 GHz, 800 K at 115 GHz, and from 400 to 800 K in the 120–150 GHz range. The image rejection ratio of the SSB filter is 20 dB. Two filter banks with 256 MHz bandwidth and 1 MHz resolution were used in serial mode to get 512 MHz band coverage. An rms noise from 0.01 to 0.03 K was achieved during the entire observation period. Pointing was checked every 2 to 3 hours by using the SiO $v = 1$, $J = 2$–1 maser line from χ Cyg within an rms accuracy of 6″. The best focus of the secondary mirror was obtained at the beginning of each observation. Selective molecules with rotational transitions in the 2 mm band, such as HC_3N and CS, were also observed in both 3 mm and 2 mm bands. The relative pointing offset between the two bands is 3″. Spectral line intensities were calibrated by the chopper-wheel method in which atmospheric attenuation and radome losses were corrected, and expressed in units of antenna temperature, T_A^*. Lines corresponding to the detected lines from CRL 2688 were also observed toward IRC +10216 in order to compare the physical and chemical characteristics of these two stars in different evolutionary stages.

3. RESULTS AND DISCUSSION

We detected 19 transitions (including blended CN $N = 1$–0 $J = 3/2$–$1/2$ transitions) of eight molecular species and two transitions of their isotopic species in the 3 mm band toward CRL 2688. Figure 1 shows the observed spectral lines from 85.25 GHz to 115.75 GHz, where an LSR velocity of −32 km s^{-1} has been assumed. The ordinate scale is antenna temperature T_A^*. The rest frequencies and observed line parameters are given in Table 1. All of these lines are assigned to known molecular species: HCN, C_2H, HNC, HC_3N, CS, CCS, CN, CO, and their isotopic species $H^{13}CN$ and ^{13}CO. There are no molecular lines which were only detected in CRL 2688 while not detected in IRC +10216. We used two catalogs for line identification. One is the Lovas catalog (Lovas 1992) which is a collection of molecular line frequencies determined from laboratory measurements, and the other is the Jet Propulsion Laboratory (JPL) catalog (Pickett et al. 1998) which is a collection of theoretical calculations of molecular lines. The CCS line was first detected in CRL 2688. Figure 2 displays the lines detected in the 85–116 GHz line survey of CRL 2688 together with corresponding lines observed from IRC +10216. All the ordinate scales are given in T_A^*. The upper spectra are from CRL 2688 and the lower spectra are from IRC +10216. LSR velocity of −26.3 km s^{-1} has been assumed for IRC +10216. The intensities of IRC +10216 spectra are scaled down to 10% of the original ones. Table 1 gives these line parameters observed from IRC +10216.

In the case of blended lines, only peak intensities are given without integrated intensities. The S/N of CRL 2688 data is worse compared with that of IRC +10216 data. Three HC_3N $J = 14$–13, $J = 15$–14, $J = 16$–15 and CS $J = 3$–2 spectra were also obtained in the 2 mm band. Detailed descriptions of selected molecules are given in the following sections.

3.1. CO, CS, and CCS

Figure 3 gives the line profiles of CO and ^{13}CO from CRL 2688 and IRC +10216. The ^{12}CO spectra of CRL 2688 and IRC +10216 show an optically thick emission with parabolic shape, while the ^{13}CO spectrum of CRL 2688 shows a partially optically thin emission with rectangular shape and that of IRC +10216 shows an optically thin and resolved emission with a double peak. The integrated intensity ratios $\int T_A^*(\mathrm{CO})\,dv$ / $\int T_A^*(^{13}\mathrm{CO})\,dv$ are 4.76 and 10.0 for CRL 2688 and IRC +10216, respectively. The observational results of Kahne et al. (1992) with the IRAM 30 m telescope showed that these values are 7.5 for CRL 2688 and 8.65 for IRC +10216, respectively. The use of these integrated intensity ratios of an optically thick to thin line may lead to lower limits of their abundance ratios. Kahne et al. (1992) reported that molecular abundance ratios CO/^{13}CO are 8 for CRL 2688 and 16 for IRC +10216 as lower limits. According to Wannier & Sahai (1987), abundance ratios of CO/^{13}CO were estimated to be 20 for CRL 2688 and 48 for IRC +10216 based on CO $J = 2$–1 observations. Because of this lower CO/^{13}CO ratio for CRL 2688 than for carbon stars (40–80), Jaminet et al. (1992) placed CRL 2688 among the J-type carbon stars. The line-center velocity and the full width at zero power of CO emission are −36.6 km s^{-1} and 39.4 km s^{-1}, respectively. So the half width is 19.7 km s^{-1} (in good agreement with Herpin et al. 2002), which corresponds to the expansion velocity of CRL 2688. The expansion velocity of IRC +10216 measured by the CO line is 15.6 km s^{-1}. For a young PPN CRL 2688, Cox et al. (2000) have detected a high-velocity gas emerging in two directions of the central star in the CO $J = 2$–1 line which is closely related to H_2 emission at 2 μm.

The spectra of CS $J = 2$–1 and $J = 3$–2 toward CRL 2688 (top panel) and IRC +10216 (bottom panel) are shown in Figure 2, respectively. The mapping observations of CS for CRL 2688 were performed by Kasuga et al. (1997) using the Nobeyama Millimeter Array with angular resolutions of 3″×3″. They reported that the emission is extended by about 15″. This value is smaller than the emitting size of other molecules such as HCN and HC_3N (larger than 20″). Their modeling of the CRL 2688 envelope indicates that the density distribution is nearly spherically symmetric but the abundance of CS is enhanced near the polar regions. According to their results, the high-velocity flow may be limited in the inner region of the envelope. Generally the CS line traces a dense region ($\geqslant 10^4$ cm^{-3}). In the case of IRC +10216, the line profile of 250 kHz resolution shows a flat-topped feature, which indicates a partially optically thin molecular shell. The line intensity of CS $J = 3$–2 from CRL 2688 is about a tenth of that from IRC +10216.

This observation is the first to detect a CCS line in CRL 2688; although this molecule has been detected in IRC +10216 (Cernicharo et al. 1987). CCS is 40 times less abundant than CS in the case of IRC +10216 (Cernicharo et al. 1987). Cernicharo et al. (1987) reported that CCS can be formed at chemical equilibrium in the outer stellar atmosphere and can also be formed further in the envelope from CS, by

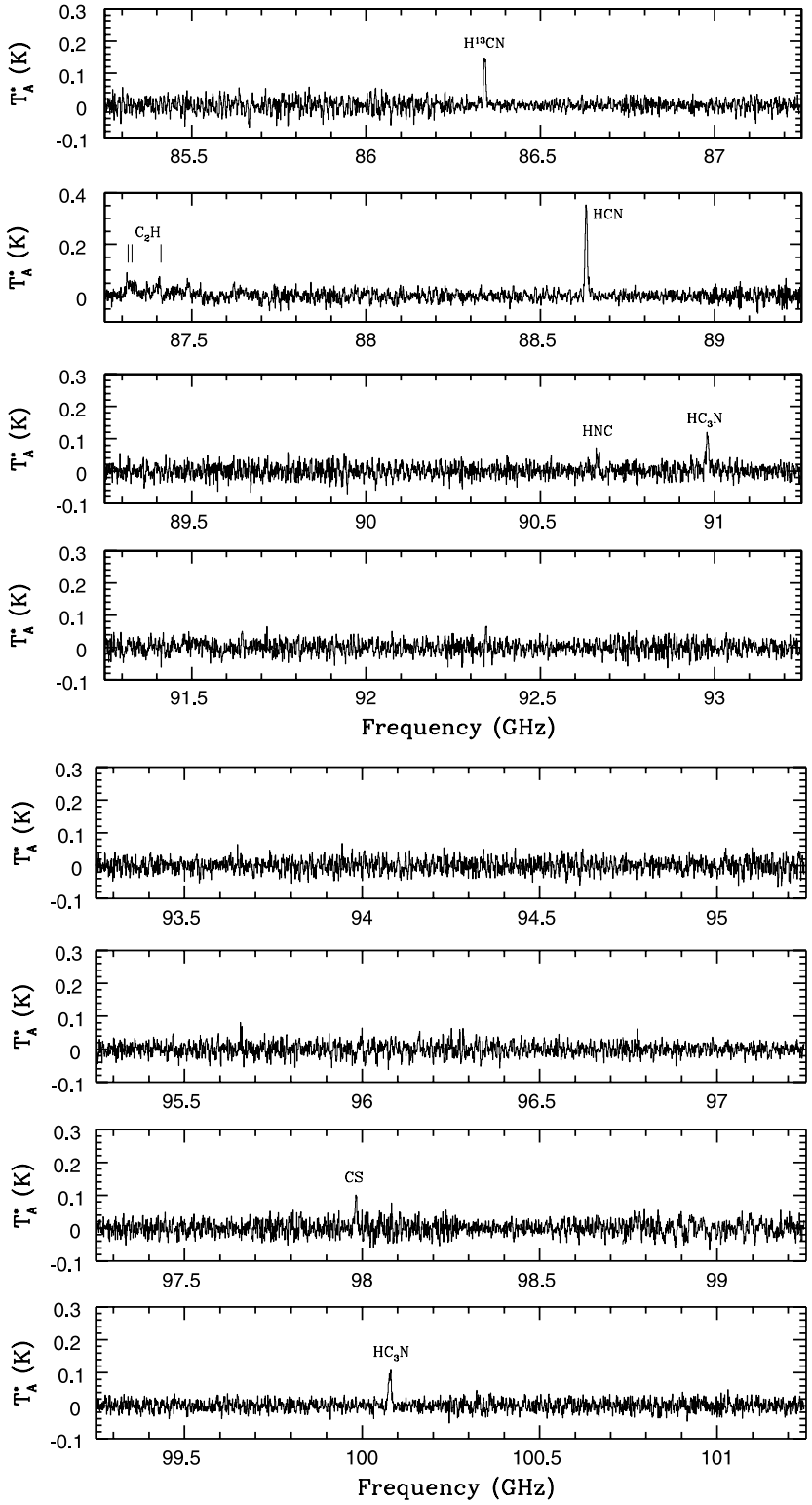

Figure 1. Total spectra of the survey of CRL 2688 ranged from 85.25 GHz to 115.75 GHz with 1 MHz resolution.
(An extended version of this figure is available in the online journal.)

ion–molecule reactions. Similar formation processes may be also applied to CRL 2688.

3.2. HCN, HNC, and HC_3N

The line profiles of HCN and $H^{13}CN$ from CRL 2688 and IRC +10216 are given in Figure 2. The integrated antenna temperature ratios of HCN to $H^{13}CN$ $\int T_A^*(\mathrm{HCN})\,dv$ / $\int T_A^*(H^{13}CN)\,dv$ are 2.24 and 2.44 for CRL 2688 and IRC +10216, respectively. The latter value, 2.44 for IRC +10216 is larger than the values 2.0, observed with the Onsala 20 m telescope (Olofsson et al. 1982), and 1.65, observed with the IRAM 30 m telescope (Kahne et al. 1988) probably due to different beam dilution factors. Nguyen-Q-Rieu & Bieging (1990) showed that the isotope ratio HCN/$H^{13}CN$ in CRL 2688 appeared to be 5 as

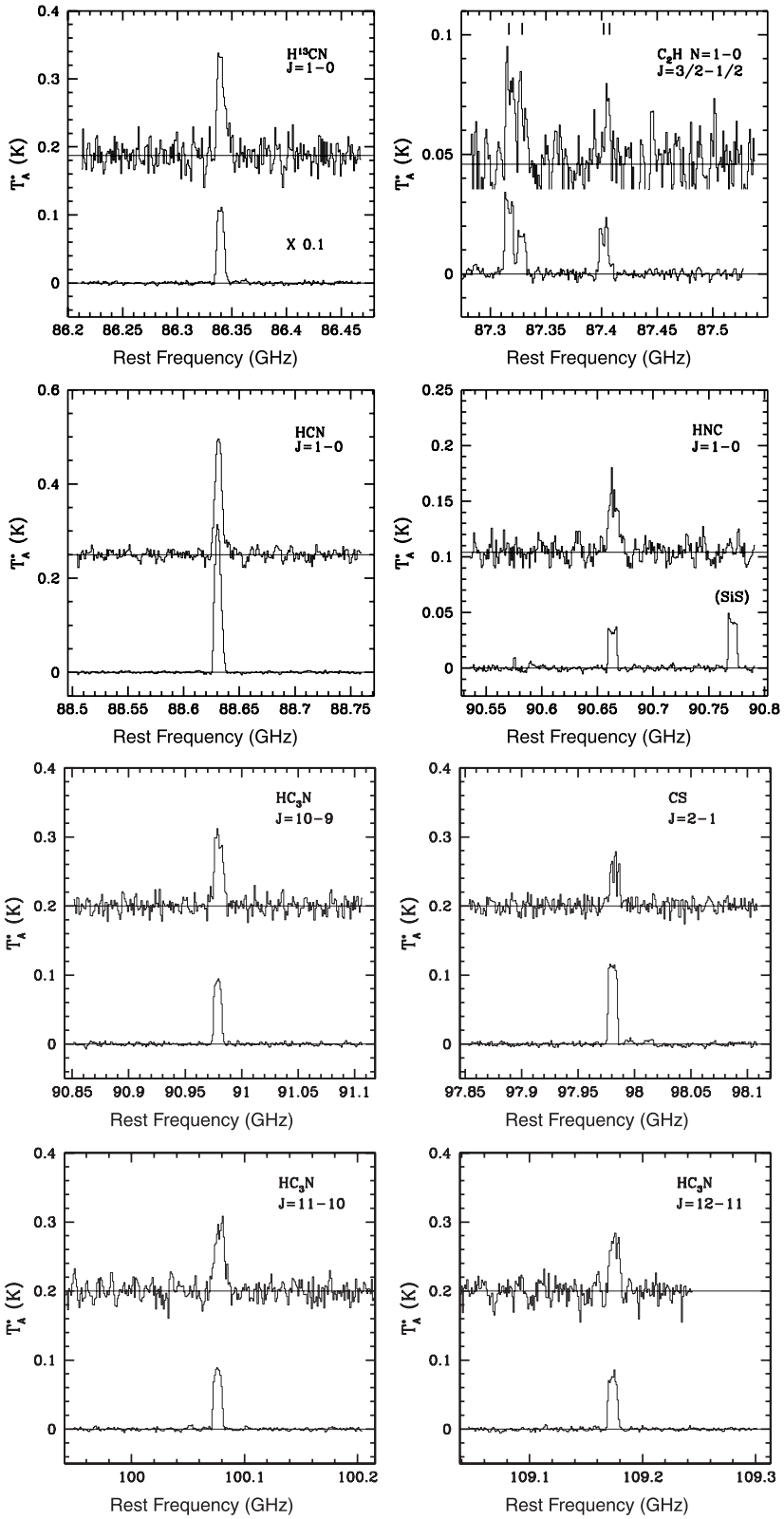

Figure 2. Spectra of CRL 2688 (top of each panel) and IRC +10216 (bottom of each panel) with 1 MHz resolution.

a lower limit for optically thick lines and that its determination is difficult because of line saturation and hyperfine line blending. Dinh-V-Trung & Nguyen-Q-Rieu (2000) reproduced the observed spectrum at the center position of IRC +10216 with a radiative transfer model of $[\mathrm{HCN}]/[\mathrm{H_2}] = 2.5 \times 10^{-5}$, given an isotopic ratio $^{12}\mathrm{C}/^{13}\mathrm{C} = 55$. The carbon isotopic ratio $^{12}\mathrm{C}/^{13}\mathrm{C}$ is an important value for understanding nucleosynthesis and the evolution stage (Iben & Renzini 1983; Balser et al. 2002), but it is difficult to determine the ratio by using optically thick lines of CO and HCN (Kwan & Hill 1977). The asymmetric features of the HCN and $\mathrm{H^{13}CN}$ spectra which may be produced by self absorption and/or blending of hyperfine components (Nguyen-

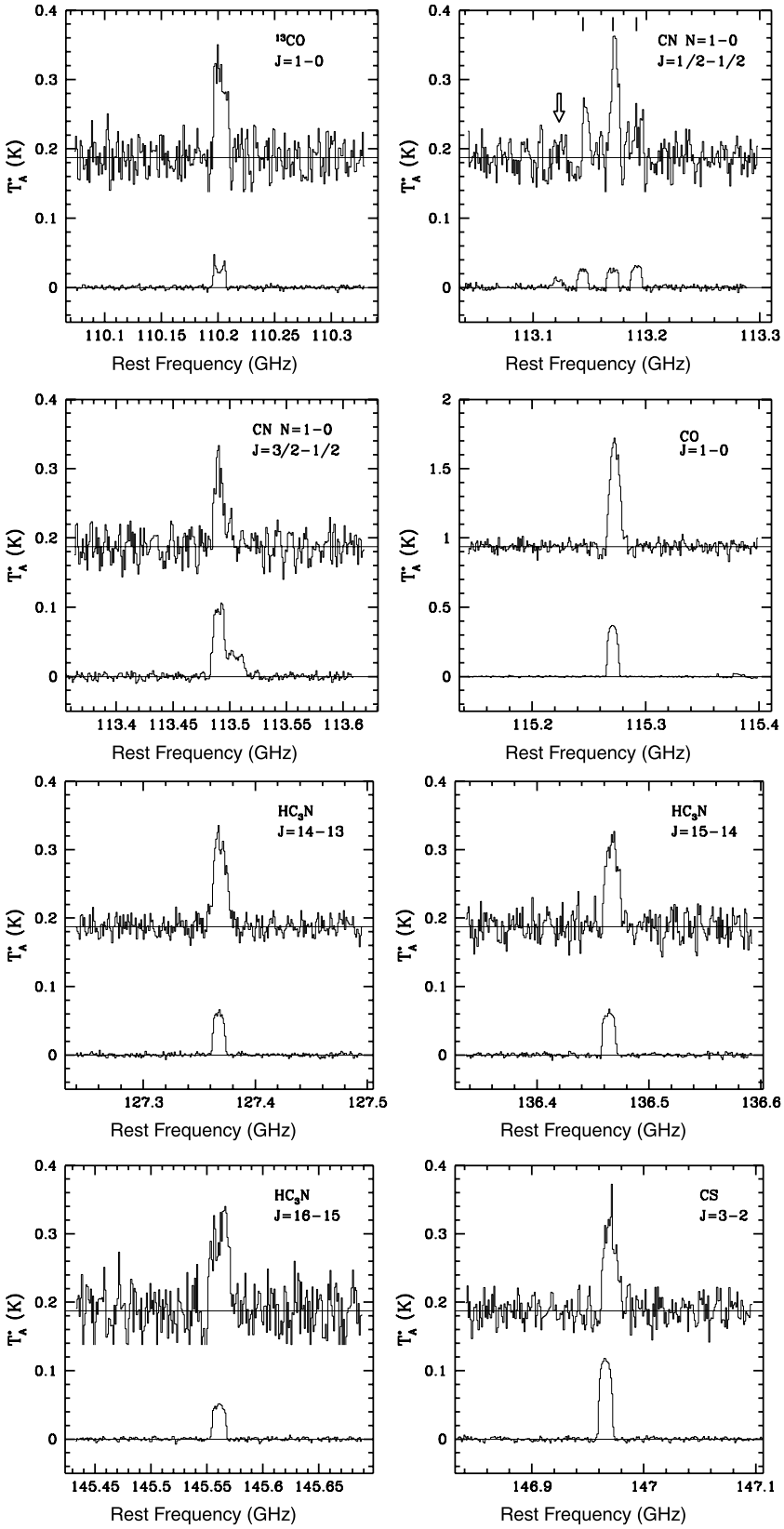

Figure 2. (Continued)

Q-Rieu et al. 1988; Nguyen-Q-Rieu & Bieging 1990; Bieging et al. 1988) were not observed in CRL 2688, unlike in IRC +10216.

As shown in Figure 2, spectra from 90.55 GHz to 90.8 GHz, the SiS ($J = 5$–4, $v = 0$) molecular line was detected in IRC +10216 while it was not detected in CRL 2688 in our

Table 1
Line Parameters Detected in CRL 2688 and Observed in IRC +10216[a]

Frequency	Mole.	Transition	CRL 2688		IRC +10216	
			T_A^*	$\int T_A^* dv$	T_A^*	$\int T_A^* dv$
(GHz)			(K)	(K km s^{-1})	(K)	(K km s^{-1})
86.3402	$H^{13}CN$	$J = 1$–0	0.16 ± 0.01	4.15 ± 0.15	1.21 ± 0.02	30.10 ± 0.23
87.3169	C_2H	$N = 1$–0 $J = 3/2$–1/2 $F = 2$–1	0.05 ± 0.02	1.76 ± 0.28	0.33 ± 0.01	9.71 ± 0.20
87.3286	C_2H	$N = 1$–0 $J = 3/2$–1/2 $F = 1$–0	0.05 ± 0.02	2.47 ± 0.31	0.18 ± 0.01	5.14 ± 0.21
87.4120	C_2H	$N = 1$–0 $J = 3/2$–1/2 $F = 1$–1	0.05 ± 0.02	5.05 ± 0.47	0.20 ± 0.01	6.01 ± 0.20
88.6318	HCN	$J = 1$–0	0.36 ± 0.01	9.24 ± 0.20	3.28 ± 0.02	72.39 ± 0.23
90.6635	HNC	$J = 1$–0	0.04 ± 0.02	1.44 ± 0.23	0.39 ± 0.02	9.82 ± 0.23
90.7715	SiS	$J = 5$–4	...	...	0.39 ± 0.02	12.44 ± 0.22
90.9790	HC_3N	$J = 10$–9	0.10 ± 0.02	3.43 ± 0.29	1.05 ± 0.02	23.83 ± 0.24
97.9810	CS	$J = 2$–1	0.10 ± 0.02	2.40 ± 0.32	1.32 ± 0.03	31.20 ± 0.31
100.0764	HC_3N	$J = 11$–10	0.10 ± 0.01	3.02 ± 0.18	0.99 ± 0.02	21.99 ± 0.21
103.6408	CCS	(J, N)=(8, 8)–(7, 7)	0.07 ± 0.02	3.64 ± 0.34	...	...
109.1736	HC_3N	$J = 12$–11	0.08 ± 0.01	2.00 ± 0.14	0.88 ± 0.02	19.75 ± 0.21
110.2014	^{13}CO	$J = 1$–0	0.14 ± 0.02	3.56 ± 0.22	0.31 ± 0.02	9.54 ± 0.28
113.1217	CN	$N = 1$–0 $J = 1/2$–1/2 $F = 1/2$–1/2	...	...	0.12 ± 0.03	2.62 ± 0.29
113.1442	CN	$N = 1$–0 $J = 1/2$–1/2 $F = 1/2$–3/2	0.05 ± 0.02	1.61 ± 0.45	0.32 ± 0.03	7.13 ± 0.30
113.1705	CN	$N = 1$–0 $J = 1/2$–1/2 $F = 3/2$–1/2	0.12 ± 0.02	2.70 ± 0.33	0.34 ± 0.03	8.39 ± 0.30
113.1913	CN	$N = 1$–0 $J = 1/2$–1/2 $F = 3/2$–3/2	0.08 ± 0.02	1.81 ± 0.31	0.39 ± 0.03	8.85 ± 0.30
113.4881	CN	$N = 1$–0 $J = 3/2$–1/2 $F = 3/2$–1/2				
113.4910	CN	$N = 1$–0 $J = 3/2$–1/2 $F = 5/2$–3/2				
113.4996	CN	$N = 1$–0 $J = 3/2$–1/2 $F = 1/2$–1/2	0.18 ± 0.03[b]	4.20 ± 0.14[b]	1.03 ± 0.06[b]	34.35 ± 0.98[b]
113.5089	CN	$N = 1$–0 $J = 3/2$–1/2 $F = 3/2$–3/2				
113.5204	CN	$N = 1$–0 $J = 3/2$–1/2 $F = 1/2$–3/2				
115.2712	CO	$J = 1$–0	0.94 ± 0.03	25.71 ± 0.53	4.16 ± 0.05	95.02 ± 0.54
127.3677	HC_3N	$J = 14$–13	0.14 ± 0.01	4.20 ± 0.14	0.70 ± 0.02	15.98 ± 0.24
136.4644	HC_3N	$J = 15$–14	0.13 ± 0.02	3.70 ± 0.20	0.70 ± 0.02	16.08 ± 0.23
145.5609	HC_3N	$J = 16$–15	0.14 ± 0.03	4.38 ± 0.34	0.57 ± 0.02	12.84 ± 0.20
146.9690	CS	$J = 3$–2	0.14 ± 0.02	3.56 ± 0.20	1.32 ± 0.03	28.41 ± 0.24

Notes.
[a] Line parameters observed in IRC +10216 corresponding to the detected lines in CRL 2688.
[b] Five hyperfine lines are blended. The line parameters are given for blended, but bright component only.

observations. We estimated an upper limit on the SiS abundance for $T_A^* \sim .06$ K (rms = 0.02 K) in CRL 2688. We assumed the source size of 35″ for the SiS $J = 5$–4 line (Fukasaku et al. 1994). The beam dilution factor was corrected. As a result, we got a column density of 2.6×10^{13} cm^{-2} and an abundance (relative to H_2) of 1.2×10^{-8}, whose orders are comparable to the results of 4.5×10^{13} cm^{-2} (Fukasaku et al. 1994) and 4×10^{-8} (Nguyen-Q-Rieu & Bieging 1990). In the case of IRC +10216, its column density and abundance were estimated to be 4.7×10^{15} cm^{-2} (Kawaguchi et al. 1995) and 6.5×10^{-7} (Nguyen-Q-Rieu & Bieging 1990), respectively. These values show a lower abundance of the SiS molecule in CRL 2688 than in IRC +10216. SiS is known to be produced in regions of chemical equilibrium. Therefore, SiS abundance decreases as a star evolves beyond the AGB, through the PPN and PN phases (Bachiller et al. 1997a). But the HNC molecule is mainly formed by ion–molecule reactions. Glassgold et al. (1987) indicated that HNC is produced from a dissociative recombination of $HCNH^+$. The higher HNC abundances in the more evolved object PPN CRL 2688 may be ascribed to a higher level of ionization in the gas originated from radiation of the central star (Fukasaku et al. 1994).

Six rotational transitions in the ground vibrational state of HC_3N were detected in our line survey toward CRL 2688. Many millimeter wave spectra produced by rotational transitions of ground and vibrationally excited states of HC_3N have been also detected from the C-rich proto-planetary nebula CRL 618 and have allowed quite a precise determination of physical conditions (Wyrowski et al. 2003; Pardo et al. 2004, 2007b). We also adopted the HC_3N lines for investigating physical conditions such as excitation temperature and column density in CRL 2688.

Rotation temperatures ($T_{\rm rot}$) and column densities (N) of HC_3N in CRL 2688 and IRC +10216 were derived using standard LTE rotational diagram analysis (Turner 1991).

The equation for the analysis is given by

$$\log L = \log \frac{3k \int T_A^* dv}{8\eta_B \pi^3 \nu S \mu_i^2 g_I g_k} = \log \frac{N}{Q_{\rm rot}} - \frac{E_u \log e}{kT_{\rm rot}}, \quad (1)$$

where k is the Boltzmann constant, $\int T_A^* dv$ is the integrated intensity, η_B is the main beam efficiency of the telescope, ν is the rest frequency of the line, S is the line strength, μ_i is the relevant dipole moment, g_I is the reduced nuclear spin weight, g_k is the K-level degeneracy, E_u is the upper state energy of the transition, $Q_{\rm rot}$ is the rotational partition function, and N is the column density.

The above equation is based upon the assumptions that lines are optically thin, level populations are characterized by a single $T_{\rm rot}$ (LTE), $T_{\rm rot} \gg T_{\rm bg}$ (background temperature), and the Rayleigh–Jeans approximation is valid for all transitions (Turner 1991). The values for g_I, g_k, E_u/k, $S\mu_i^2$, $\log L$, and η_B for HC_3N are given in Table 2. The partition function $Q_{\rm rot}$ for this molecule is given by $3[kT_{\rm rot}/hB]$ (Blake et al. 1986), where B is the rotational constant (4549.059 MHz from Lafferty & Lovas 1978). In total, six rotational transitions were detected

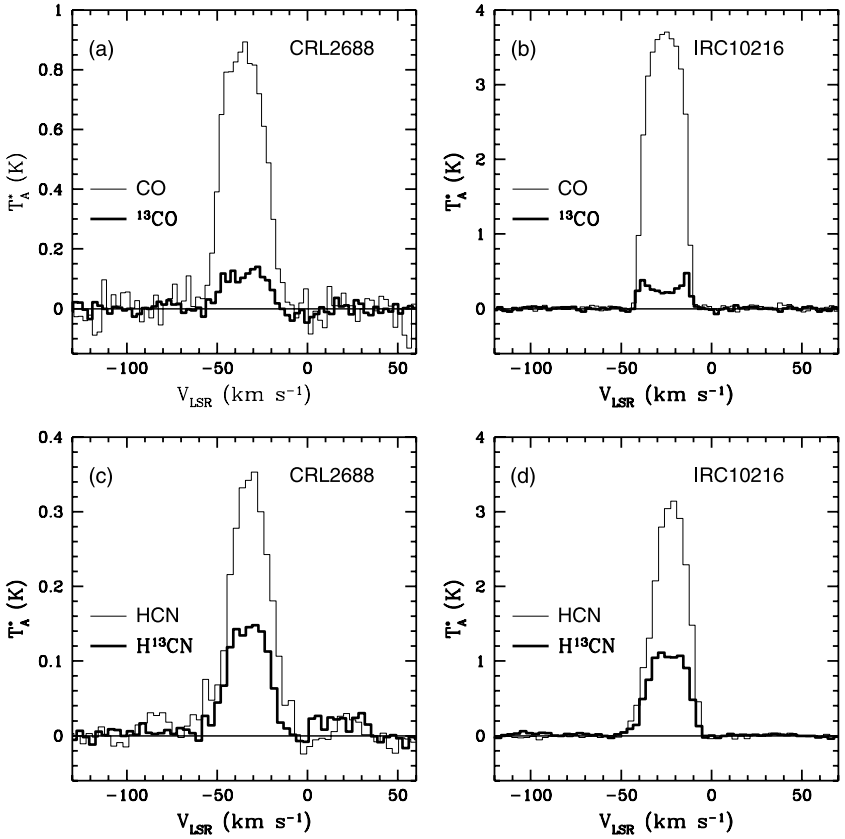

Figure 3. Spectra of CO $J = 1$–0, ^{13}CO $J = 1$–0, HCN $J = 1$–0, and H^{13}CN $J = 1$–0 in CRL 2688 and IRC +10216.

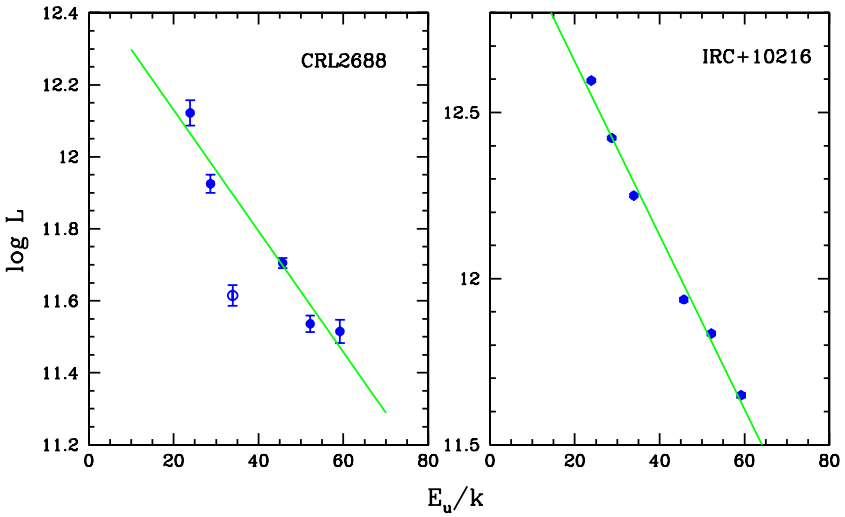

Figure 4. Rotation diagrams for the HC_3N molecule. The datum marked with an open circle in CRL 2688 is excluded in the least-squares fit because of a calibration problem. Error bars are included within dot marks in the case of IRC +10216 because the relative ratio between integrated intensity and their errors is very small.

(A color version of this figure is available in the online journal.)

in CRL 2688 and IRC +10216 (Table 1). Observed antenna temperatures were converted to source brightness temperature (T_R), where we considered the effect of main beam efficiency (η_B) and beam dilution (η_{BD}) as follows,

$$T_R = T_A^*/\eta_B\eta_{BD}.$$

The correction factor for beam dilution is calculated using

$$\eta_{BD} = [1 + (\theta_B/\theta_S)^2]^{-1},$$

where θ_B is the antenna beam width (FWHM) and θ_S is the source diameter (Bell 1993). We assumed that the source size of 20″ is uniform with our observing frequencies as Fukasaku et al. (1994) adopted. The beam size was obtained from an interpolation using the values, 64″ at 84 GHz and 46″ at 150 GHz. In the case of CRL 2688, all HC_3N data except for $J = 12$–11 were found to be in a good linear correlation in the distribution of E_u/k versus log L, as shown in Figure 4. This good correlation, except for the $J = 12$–11 transition datum, confirms the validity of the above assumptions for LTE rotation diagram analysis. The datum of the $J = 12$–11 transition probably has a calibration problem. Therefore, excluding the $J = 12$–11 transition datum, we made a linear least-squares fit and found $T_{ex} = 25.8^{+3.5}_{-2.7}$ K

Table 2
Line Parameters Used in Calculation of Excitation Temperatures and Column Densities of HC_3N

Frequency (MHz)	Transition $J(K_{-1}, K_{+1})$	g_I	g_k	E_u/k [a] (K)	$S\mu^2$ [a] (Debye^2)	η_B [b]
90979.0	$J = 10$–9	1	1	23.9	100	0.49
100076.4	$J = 11$–10	1	1	28.7	121	0.48
109173.6	$J = 12$–11	1	1	33.9	144	0.47
127367.7	$J = 14$–13	1	1	45.7	196	0.43
136464.4	$J = 15$–14	1	1	52.2	225	0.41
145560.9	$J = 16$–15	1	1	59.2	256	0.39

Notes.
[a] From Lafferty & Lovas (1978).
[b] The main beam efficiencies are 0.5 at 86 GHz and 0.39 at 146 GHz from Park et al. (1997). The rest values are inferred from these two values.

Table 3
Excitation Temperature and Column Densities of HC_3N in CRL 2688 and IRC +10216

	Present Work		Other Study	
	T_{ex} (K)	N (cm^{-2})	T_{ex} (K)	N (cm^{-2})
CRL 2688	25.8	3.5×10^{14}	83[a]	7.3×10^{14}[a]
IRC +10216	16.6	1.1×10^{15}	26[b]	1.7×10^{15}[b]

Notes.
[a] Fukasaku et al. (1994).
[b] Kawaguchi et al. (1995).

and $N = 3.5^{+1.4}_{-1.0} \times 10^{14}$ cm^{-2}. In the case of IRC +10216, all data in the distribution of E_u/k versus log L were found to be in a good linear correlation. From the least-squares fit, we have also derived $T_{ex} = 16.6^{+0.9}_{-0.8}$ K, and $N = 1.1^{+0.2}_{-0.2} \times 10^{15}$ cm^{-2}. These results along with literature values are given in Table 3. The HC_3N column density derived by us is consistent with the value in Fukasaku et al. (1994) within a factor of ~ 2. Bachiller et al. (1997) also showed that the HC_3N column density is estimated to be 4.4×10^{14}cm^{-2} in CRL 2688. The observed HC_3N line shapes in CRL 2688 have showed an optically thick profile (Fukasaku et al. 1994) or, at least a partially optically thick profile (Olofsson et al. 1982) conflicting with the optically thin assumption above. Therefore, in order to confirm a better accurate optical depth of HC_3N in CRL 2688, it might be necessary to observe the isotope line of HC_3N by using a high-sensitivity radio telescope. The HC_3N column density of CRL 2688 estimated by us is lower than that of IRC +10216, as shown in Table 3. Nguyen-Q-Rieu & Bieging (1990) and Bieging & Tafalla (1993) also showed that HC_3N abundance relative to H_2 is lower in CRL 2688 than in IRC +10216 although Bujarrabal et al. (1988) did not find a difference in HC_3N abundance between CRL 2688 and IRC +10216. These facts may be related to the chemical evolution of the circumstellar envelopes of AGB stars. Specifically, Bachiller et al. (1997a) suggested that, as a star evolves beyond the AGB, through the proto-planetary and planetary phases, the abundance of HC_3N as well as the abundance of SiO, SiC_2, and CS decreases and HC_3N is not detected in the planetary nebulae.

3.3. C_2H and CN

The C_2H and CN radicals are known to be extended to 50″ and 75″ in IRC +10216, respectively (Truong-Bach et al. 1987). Three hyperfine components of the $N = 1$–0 $J = 3/2$–$1/2$ spectra of C_2H were detected in both CRL 2688 and IRC +10216, as shown in Figure 2. The ethynyl radical, C_2H, was first detected in interstellar clouds by Tucker et al. (1974). It is known that the penetrating interstellar UV field plays a major role in dissociating HCN and C_2H_2 in the inner layer and producing CN and C_2H in the outer layer. In addition, these exotic molecules will cause the syntheses of linear long carbon chain molecules $HC_{2n+1}N$ (Cyanopolynes with $n = 1, 2, 3,\ldots$). One of these, HC_3N, was detected in six rotational transitions in this survey.

The $N = 1$–0 transitions of CN molecule with nine hyperfine components forming two fine-structure groups ($J = 1/2$–$1/2$ and $J = 3/2$–$1/2$) are shown in Table 1 and in Figure 2. The $N = 1$–0 $J = 3/2$–$1/2$ spectra of CN show a blended feature in both IRC +10216 and CRL 2688. The weakest component of the four $N = 1$–0 $J = 1/2$–$1/2$ spectra of CN (arrow mark in the CN $N = 1$–0 $J = 1/2$–$1/2$ spectrum of Figure 2) is not seen in the case of CRL 2688 because of lower sensitivity of the TRAO 14 m telescope compared with the IRAM 30 m telescope although all the four spectra of CN were detected by Bachiller et al. (1997a, 1997b). Bachiller et al. (1997a, 1997b) reported that the CN/HCN abundance ratio is 2 in CRL 2688 compared to about 0.5 in C-rich AGB envelopes including IRC +10216. This large abundance of CN in CRL 2688 may be related to the effect of chemistry influenced by the UV radiation of the central star during the PPN phase (Kwok 2000).

4. CONCLUSION

We have carried out a spectral line survey from 85 GHz to 116 GHz together with 2 mm band line observations of HC_3N and CS toward the PPN CRL 2688. The eight detected molecules were all carbon-bearing molecules: HCN, HNC, C_2H, HC_3N, CS, CCS, CN, and CO, and their isotopic species $H^{13}CN$ and ^{13}CO. A CCS line was detected in CRL 2688 for the first time. The detected lines in this survey of CRL 2688 were also observed toward the proto-typical AGB star IRC +10216 and the observational characteristics of the two sources were investigated. From the observed CO line profiles, the center velocity and the expansion velocity of both sources were obtained. The expansion velocity of CRL 2688 is 19.7 km s^{-1} which is larger than that of IRC +10216 (15.6 km s^{-1}). The asymmetric features of the HCN and $H^{13}CN$ spectra were not shown in CRL 2688, unlike in IRC +10216. The molecules of C_2H and CN have hyperfine structures whose lines often appear to be blended. The HNC line profile of CRL 2688

showed an optically thick feature with a parabolic shape, while that of IRC +10216 showed an optically thin feature with a double peak. The SiS (J = 5–4, v = 0) molecular line was detected in IRC +10216, while it was not detected in CRL 2688, indicating a lower abundance of the SiS molecule in CRL 2688. N = 1–0 transitions of the CN molecule consisted of nine hyperfine components forming two fine-structure groups (J = 1/2–1/2 and J = 3/2–1/2) and were detected in both IRC +101216 and CRL 2688. But one of the four N = 1–0 J = 1/2–1/2 spectra of CN was not seen in the case of CRL 2688. The N = 1–0 J = 3/2–1/2 spectra of CN showed a blended feature in both IRC +10216 and CRL 2688.

Using standard LTE rotational diagram analysis, excitation temperatures (T_{ex}) and column densities (N) of HC_3N in CRL 2688 and IRC +10216 were derived. We found $T_{ex} = 35.3^{+6.5}_{-4.7}$ K and $N = 3.6^{+0.5}_{-0.3} \times 10^{13}$ cm^{-2} in CRL 2688 and $T_{ex} = 20.1^{+1.3}_{-1.1}$ K, $N = 2.3^{+0.5}_{-0.4} \times 10^{14}$ cm^{-2} in IRC +10216, respectively. The HC_3N column density of CRL 2688 was found to be lower than that of IRC +10216. This fact, together with the lower abundance of the SiS molecule in CRL 2688, may be related to the chemical evolution of the circumstellar envelope of the proto-planetary nebula CRL 2688 beyond the AGB star as Bachiller et al. (1997a) suggested.

This work was supported by the National Strategic R&D Program (1999–2001) and the Basic Research Program (2007) of the Korea Astronomy and Space Science Institute, which is sponsored by the Ministry of Science and Technology of Korea. C.W.L. acknowledges support by the KOSEF R01-2004-000-10513-0 program and J.Y. acknowledges support by the Korea Research Foundation Grant funded by the Korean Government (MOEHRD) (KRF-2007-341-C00020). We are also grateful to the anonymous referee for useful indications that led to improvement of this paper.

REFERENCES

Avery, L. W., et al. 1985, A&AS, 60, 135
Avery, L. W., et al. 1992, ApJS, 83, 363
Bachiller, R., Forveille, T, Huggins, P. J., & Cox, P. 1997a, A&A, 324, 1123
Bachiller, R., Fuente, A., Bujarrabal, V., Colomer, F., Loup, C., Omont, A., & de Jong, T. 1997b, A&A, 319, 235
Balser, D. S., McMullin, J. P., & Wilson, T. L. 2002, ApJ, 572, 326
Bell, M. B. 1993, ApJ, 417, 305
Bieging, J. H., & Nguyen-Q-Rieu, 1988, ApJ, 324, 516
Bieging, J. H., & Tafalla, M. 1993, AJ, 105, 576
Blake, G. A., Sutton, E. C., Masson, C. R., & Phillips, T. G. 1986, ApJS, 60, 357
Bujarrabal, V., Gomez-Gonzalez, J., Bachiller, R., & Martin-Pintado, J. 1988, A&A, 204, 242
Cernicharo, J., Guelin, M., Hein, H., & Kahane, C. 1987, A&A, 181, L9
Cernicharo, J., Guelin, M., & Kahane, C. 2000, A&AS, 142, 181
Cernicharo, J., Heras, A. M., Tielens, A. G. G., Pardo, J. R., Herpin, F., Guelin, M., & Waters, L. B. F. M. 2001, ApJ, 546, L123
Cox, P., Lucas, R., Huggins, P. J., Forveille, T., Bachiller, R., Guilloteau, S., Maillard, J. P., & Omont, A. 2000, A&A, 353, L25
Dinh-V-Trung, & Nguyen-Q-Rieu, 2000, A&A, 361, 601
Fukasaku, S., Hirahara, Y., Masuda, A., Kawaguchi, K., Ishikawa, S., Kaifu, N., & Irvine, W. 1994, ApJ, 437, 410
Glassgold, A. E., Mamon, G. A., Omont, A., & Lucas, R. 1987, A&A, 180, 183
Groesbeck, T. D., Phillips, T. G., & Blake, G. A. 1994, ApJS, 94, 147
Herpin, F., & Cernicharo, J. 2000, ApJ, 530, L129
Herpin, F., Goicoechea, J. R., Pardo, J. R., & Cernicharo, J. 2002, ApJ, 577, 961
Highberger, J. L., Thomson, K. J., Young, P. A., Arnett, D., & Ziurys, L. M. 2003, ApJ, 593, 393
Iben, I., Jr., & Renzini, A. 1983, ARA&A, 21, 271
Jaminet, P. H., Danchi, W. C., Sandell, G., & Sutton, E. C. 1992, ApJ, 400, 535
Jewell, P. R., & Snyder, L. E. 1984, ApJ, 278, 176
Johnansson, L. E. B., Andersson, C., Ellder, J., Friberg, P., Hjalmason, A., Hoglund, B., Irvine, W. M., & Olofsson, H. 1985, A&AS, 60, 135
Kahne, C., Cernicharo, J., Gomez-Gonzalez, J., & Guelin, M. 1992, A&A, 256, 235
Kahne, C., Gomez-Gonzalez, J., Cernicharo, J., & Guelin, M. 1988, A&A, 190, 167
Kasuga, T., Yamamura, I., & Deguchi, S. 1997, A&A, 320, 575
Kawaguchi, K., Kasai, Y., Ishikawa, S., & Kaifu, N. 1995, PASJ, 47, 853
Kim, H. D., Cho, S. H., Chung, H. S., Kim, H. R., Roh, D. G., Kim, H. G., Minh, Y. C., & Minn, Y. K. 2000, ApJS, 131, 483
Kim, H. D., Cho, S. H., Lee, C. W., & Burton, M. G. 2001, JKAS, 34, 167
Knapp, G. R., & Morris, M. 1985, ApJ, 292, 640
Kwan, J., & Hill, F. 1977, ApJ, 215, 781
Kwok, S. 2000, in The Origin and Evolution of Planetary Nebulae (Cambridge: Cambridge Univ. Press)
Lafferty, W. J., & Lovas, F. J. 1978, J. Phys. Chem. Ref. Data, 7(2), 441
Lee, C. W., Cho, S. H., & Lee, S. M. 2001, ApJ, 551, 333
Lee, C. W., & Cho, S. H. 2002, JKAS, 35, 187
Lovas, F. J. 1992, Web Version 1.0, Release date: April 1996; Published Version Recommended Rest Frequencies for Observed Interstellar Molecular Microwave Transitions—1991 Revision J. Phys. Chem. Ref. Data 21(2), 181
Lucas, R., Omont, R., Guilloteau, S., & Nguyen-Q-Rieu, 1986, A&A, 154, L12
Nguyen-Q-Rieu, & Bieging, J. H. 1990, ApJ, 359, 131
Nguyen-Q-Rieu , Deguchi, S., Izumiura, H., Kaifu, N., Ohishi, M., Suzuki, H., & Ukita, N. 1988, ApJ, 330, 374
Ney, E. P., Merrill, K. M., Becklin, E. E., Neugebauer, G., & Wynn-Williams, C. G. 1975, ApJ, 198, L129
Olofsson, H., Johansson, L. E. B., Hjalmarson, A., & Nguyen-Q-Rieu, 1982, A&A, 107, 128
Pardo, J. R., & Cernicharo, J. 2007a, ApJ, 654, 978
Pardo, J. R., Cernicharo, J., Goicochea, J. R., Guelin, M., & Ramos, A. A. 2007b, ApJ, 661, 250
Pardo, J. R., Cernicharo, J., Goicochea, J. R., & Phillips, T. G. 2004, ApJ, 615, 495
Park, J. A., et al. 1999, Int. J. of IR & mm waves, 20, 1769
Park, Y. S., Nam, U. W., Lee, C. H., Kim, T.-S., Kim, H. R., Han, S. T., & Kim, K. D. 1997, Int. J. of IR & mm waves, 18, 1565
Pickett, H. M., Poynter, R. L., Cohen, E. A., Delitsky, M. L., Pearson, J. C., & Muller, H. S. P. 1998, J. Quant. Spectrosc. & Radiat. Transfer, 60, 883
Sahai, R., et al. 1998, ApJ, 493, 301
Sanchez-Contreras, C., & Sahai, R. 2004, ApJ, 602, 960
Truong-Bach , Graham, D., & Nguyen-Q-Rieu, 1988, A&A, 199, 291
Truong-Bach , Graham, D., & Nguyen-Q-Rieu, 1993, A&A, 277, 133
Truong-Bach, Nguyen-Q-Rieu, Omont, A., Olofsson, H., & Johansson, L. E. B. 1987, A&A, 176, 285
Turner, B. E. 1991, ApJS, 76, 617
Tucker, K. D., Kutner, M. L., & Thaddeus, P. 1974, ApJ, 193, L115
Wannier, P. G., & Sahai, R. 1987, ApJ, 319, 367
Wyrowski, F., Schilke, P., Thorwirth, S., Menten, K. M., & Winnewisser, G. 2003, ApJ, 586, 344